NATIONAL ADVISORY COMMITTEE FOR AERONAUTICS

TECHNICAL NOTE

No. 1369

JUL 21 1947

EFFECT OF GEOMETRIC DIHEDRAL ON THE AERODYNAMIC CHARACTERISTICS OF TWO ISOLATED VEE-TAIL SURFACES

By Robert O. Schade

Langley Memorial Aeronautical Laboratory
Langley Field, Va.

FOR REFERENCE

NOT TO BE TAKEN FROM THIS ROOM

Washington
July 1947

NACA LIBRARY
LANGLEY MEMORIAL AERONAUTICAL
LABORATORY
Langley Field, Va.

NASA Technical Library
3 1176 01425 8470

NATIONAL ADVISORY COMMITTEE FOR AERONAUTICS

TECHNICAL NOTE NO. 1369

EFFECT OF GEOMETRIC DIHEDRAL ON THE AERODYNAMIC CHARACTERISTICS OF TWO ISOLATED VEE-TAIL SURFACES

By Robert O. Schade

SUMMARY

Force tests of two isolated vee-tail surfaces with various amounts of dihedral were made to provide an experimental verification of a simplified vee-tail theory and the results are presented which were found to be in good agreement with calculations of NACA ACR No. L5A03. The tails had aspect ratios of 3.70 and 5.55 and were tested with dihedral angles of 0° to 50° and 0° to 59°, respectively. Plots of the basic test data and summaries of the data in the form of plots of the variation of static-stability derivatives and control-effectiveness parameters with dihedral angle are included.

INTRODUCTION

In reference 1 a simplified vee-tail theory was presented which included a correlation with experimental data for two isolated tail surfaces having various amounts of dihedral. These experimental data consisted of lift and lateral-force parameters which were based on slopes and increments obtained from plots of force-test results. Because of the recently increased interest in vee tails, the complete force-test results including moment data which were not previously given are presented herein. These results include plots of all the basic force-test data and summaries of the data in the form of plots of the variation of different force and moment parameters with dihedral angle. The experimental data are correlated with calculations based on the simplified vee-tail theory of reference 1.

SYMBOLS

The relation of the angles and force coefficients for the vee tail in pitch and sideslip are shown in figure 1.

C_L lift coefficient (Lift/qS)

C_Y lateral-force coefficient (Y/qS)

C_l rolling-moment coefficient (L/qSb)

C_m pitching-moment coefficient $(M/qS\bar{c})$

C_n yawing-moment coefficient (N/qSb)

Y lateral force

L rolling moment

M pitching moment

N yawing moment

q dynamic pressure $\left(\frac{1}{2}\rho V^2\right)$, pounds per square foot

S actual area (not projected), square feet

$\bar{c}$ mean geometric chord, feet

b actual span (not projected), feet

V airspeed, feet per second

ρ mass density of air, slugs per cubic foot

α angle of attack of chord line at plane of symmetry, degrees

ψ angle of yaw, degrees

β angle of sideslip, degrees $(-\psi)$

δ_e elevator deflection or elerudder deflection when elerudder surfaces are deflected upward or downward together, positive when both surfaces are down, degrees

δ_r rudder deflection or elerudder deflection when elerudder surfaces are deflected equal and opposite amounts on the two sides, positive when right surface is up and left surface is down, degrees

Γ dihedral angle of tail surface measured from XY-plane of vee tail to each tail panel, degrees

τ control-effectiveness parameter $\left(\frac{\partial C_{l_N}}{\partial \delta} \Big/ \frac{\partial C_{l_N}}{\partial \alpha_N}\right)$

α_N angle of attack measured in plane normal to chord plane of each tail panel, degrees

C_{L_N} tail lift coefficient for uniform angle of attack on tail at $\beta = 0^\circ$ (sum of lifts measured in planes normal to chord planes of each tail panel as shown in fig. 1(c))

C_{L_N}' sum of changes in tail lift coefficient without regard to sign when tail is yawed at $\alpha = 0^\circ$ (one-half of lift is measured in plane normal to each tail panel as shown in fig. 1(d); equal and opposite span load distributions overlap so that $C_{L_N}' = KC_{L_N}$)

K ratio of sum of lifts obtained by equal and opposite changes in angle of attack of two semispans of tail to lift obtained by an equal change in angle of attack for complete tail

C_{L_α} rate of change of lift coefficient with angle of attack, per degree $\left(\frac{\partial C_L}{\partial \alpha}\right)$

$C_{L_{\delta_e}}$ rate of change of lift coefficient with elevator deflection, per degree $\left(\frac{\partial C_L}{\partial \delta_e}\right)$

C_{Y_β} rate of change of lateral-force coefficient with angle of sideslip, per degree $\left(\frac{\partial C_Y}{\partial \beta}\right)$

$C_{Y_{\delta_r}}$ rate of change of lateral-force coefficient with rudder deflection, per degree $\left(\frac{\partial C_Y}{\partial \delta_r}\right)$

C_{m_α} rate of change of pitching-moment coefficient with angle of attack, per degree $\left(\frac{\partial C_m}{\partial \alpha}\right)$

$C_{m_{\delta_e}}$ rate of change of pitching-moment coefficient with elevator deflection, per degree $\left(\frac{\partial C_m}{\partial \delta_e}\right)$

C_{l_β} rate of change of rolling-moment coefficient with angle of sideslip, per degree $\left(\frac{\partial C_l}{\partial \beta}\right)$

C_{n_β} rate of change of yawing-moment coefficient with angle of sideslip, per degree $\left(\frac{\partial C_n}{\partial \beta}\right)$

$C_{L_{\alpha_N}}$ slope of tail lift curve in pitch measured in plane normal to chord plane of each tail

$C_{n_{\delta_r}}$ rate of change of yawing-moment coefficient with rudder deflection, per degree $\left(\frac{\partial C_n}{\partial \delta_r}\right)$

$C_{l_{\delta_r}}$ rate of change of rolling-moment coefficient with rudder deflection, per degree $\left(\frac{\partial C_l}{\partial \delta_r}\right)$

APPARATUS, MODELS, AND TESTS

The force tests of two isolated vee tails were made on the Langley free-flight tunnel six-component balance described in reference 2. The balance rotates with the model in yaw so that all forces and moments are measured with respect to the stability axes. A sketch of the stability axes showing the positive direction of moments and forces is given as figure 2.

The two isolated-tail-surface models are shown in figure 3. Tail A had an aspect ratio of 5.55 and taper ratio of 0.39 and tail B had an aspect ratio of 3.70 and taper ratio of 0.56. The tails were hinged at the root chord to permit variation of the dihedral angle, and streamline fairings were added to simulate the rear part of a fuselage. The dihedral angles were set at 0°, 19.5°, 38.8°, 51.5°, and 59.1° for tail A and were set 0°, 30.0°, 39.8°, and 50.3° for tail B.

Force tests were made of the two tails with various amounts of dihedral, with elevator deflections of 0°, 10°, and -10°, and with rudder deflections of 0° and 10°. The tests were made at a dynamic

pressure of 4.1 pounds per square foot, which corresponds to an airspeed of about 40 miles per hour and to test Reynolds numbers of 199,000 for tail A and 256,000 for tail B based on the mean geometric chords of the tails.

The coefficients are based on true area, span, and mean geometric chord of the tail surfaces. The rolling and yawing moments are referred to axes intersecting at a point 25 percent of the root chord for each tail. The pitching moments are referred to the 25-percent point of the mean geometric chord for each tail and for each dihedral angle to permit correlation of the experimental results with calculations based on simple trigonometric relations.

CALCULATIONS

Calculations were made of the variation of some of the stability and control parameters with dihedral angle. The formulas used for calculating C_{L_α}, $C_{L_{\delta_e}}$, C_{Y_β}, and $C_{Y_{\delta_r}}$ correspond to formulas (5), (6), (7), and (8), respectively, of reference 1. In using these formulas $C_{L_{\alpha_N}}$ was assumed to be equal to $\left(C_{L_\alpha}\right)_{\Gamma=0^\circ}$ and $C_{L_{\alpha_N}}\tau$ equal to $\left(C_{L_{\delta_e}}\right)_{\Gamma=0^\circ}$. The constants K of 0.7 for tail A and 0.67 for tail B were obtained from figure 2 of reference 1.

The formulas for C_{m_α} and $C_{m_{\delta_e}}$ are based on the formulas for C_{L_α} and $C_{L_{\delta_e}}$, respectively. The variation of C_{l_β} with dihedral angle was estimated by the empirical formula

$$C_{l_\beta} = \sin\Gamma \left(\frac{C_{l_{\delta_r}}}{\tau}\right)_{\Gamma=0^\circ}$$

The control-effectiveness parameter τ was obtained from the ratio of $C_{L_{\delta_e}}$ to C_{L_α} for the 0° dihedral condition. No simple empirical relationship could be formulated for the variation of C_{n_β} and $C_{n_{\delta_r}}$ with dihedral, therefore, no calculations were made for these parameters. It was assumed that $C_{l_{\delta_r}}$ would not vary with dihedral angle except in cases of interference between the two sides of the tail.

RESULTS AND DISCUSSION

The basic force-test data are presented in figures 4 to 6 for tail A and in figures 7 to 9 for tail B. Figures 10 and 11 show a comparison of calculated and measured values of stability and control parameters for both tails. The measured values of the stability parameters were obtained from the slopes of the curves in figures 4 to 9 and the values of the control parameters were taken as the increments between the curves for different control deflections in these figures.

In general, the agreement between the calculated and experimental data of figures 10 and 11 is fairly good except at the high dihedral angles where interference between the two panels of the vee tail occurs. A comparison of the data of C_{L_α} and C_{Y_β} shows that at the high dihedral angles the vee tail is more effective in pitch and less effective in sideslip than the calculations indicate. The C_{l_β} data also show lower measured effectiveness in sideslip than the calculations indicate at the high dihedral angles. The values of C_{n_β} and $C_{n_{\delta_r}}$ increase with increasing dihedral angle but there is no consistent variation of $C_{l_{\delta_r}}$ with dihedral.

Langley Memorial Aeronautical Laboratory
National Advisory Committee for Aeronautics
Langley Field, Va., May 20, 1947

REFERENCES

1. Purser, Paul E., and Campbell, John P.: Experimental Verification of a Simplified Vee-Tail Theory and Analysis of Available Data on Complete Models with Vee Tails. NACA ACR No. L5A03, 1945.

2. Shortal, Joseph A., and Draper, John W.: Free-Flight-Tunnel Investigation of the Effect of the Fuselage Length and the Aspect Ratio and Size of the Vertical Tail on Lateral Stability and Control. NACA ARR No. 3D17, 1943.

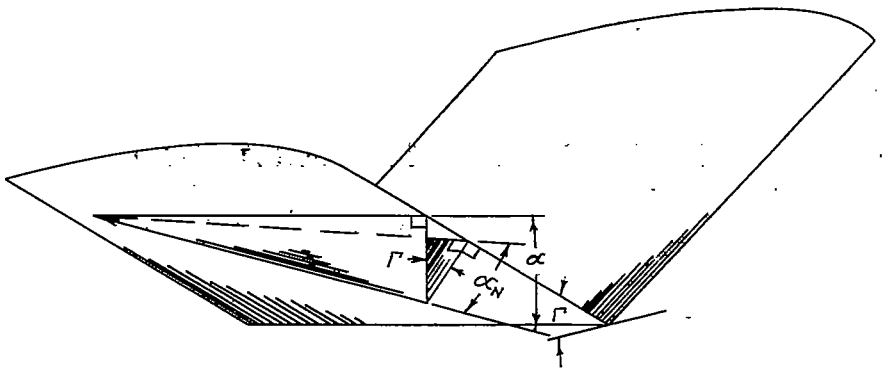

(a) Vee tail in pitch; $\beta = 0°$. If α is small, $\alpha_N = \alpha \cos \Gamma$.

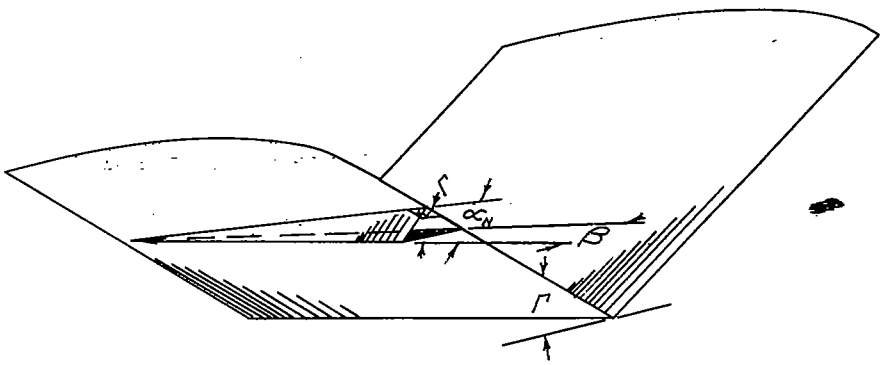

(b) Vee tail in sideslip; $\alpha = 0°$. If β is small, $\alpha_N = \beta \sin \Gamma$.

NATIONAL ADVISORY
COMMITTEE FOR AERONAUTICS

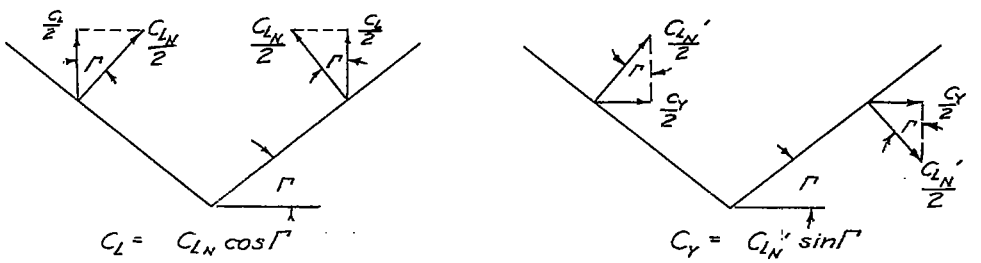

(c) Vee tail in pitch. (d) Vee tall in sideslip.

Figure I. - Relations of angles and force coefficients for vee tail in pitch and sideslip.

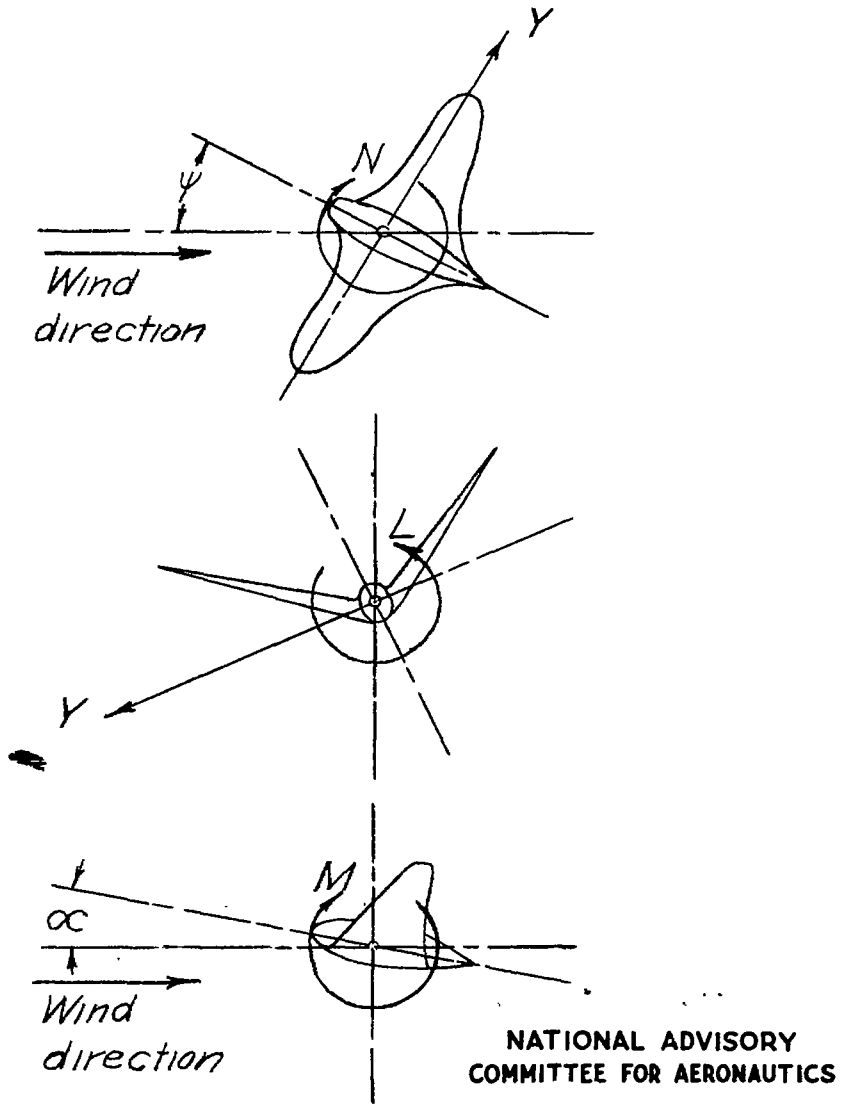

Figure 2.- The stability system of axes. This system of axes is defined as an orthogonal system in which the Z-axis is in the plane of symmetry and perpendicular to the relative wind, the X-axis is in the plane of symmetry and perpendicular to the Z-axis, and the Y-axis is perpendicular to the plane of symmetry. Arrows indicate positive directions of moments and forces.

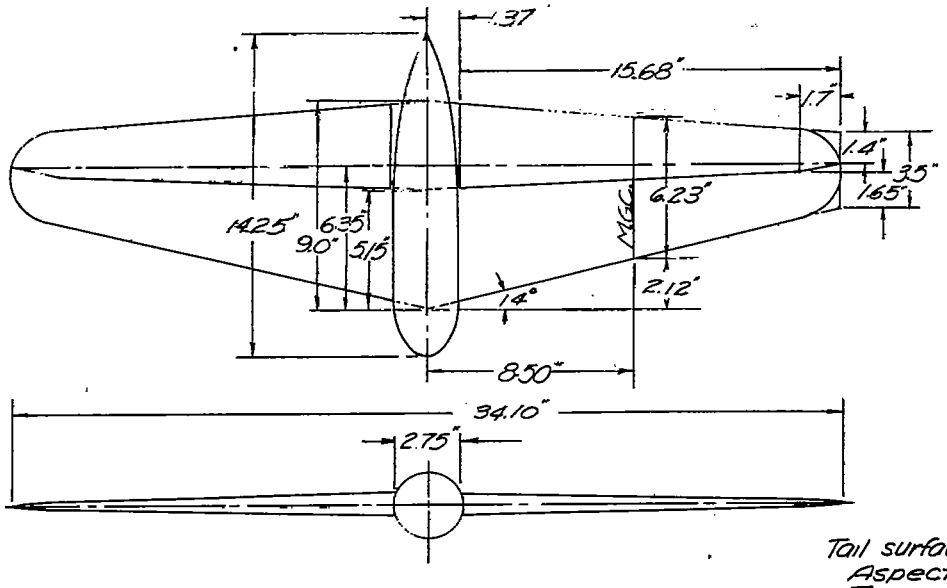

Tail surface A
Aspect ratio = 5.55
Taper ratio = 0.39
Area = 1.48 sq ft
Control-surface area behind hinge line = 0.43 sq ft
Airfoil section, NACA 0012
Dihedral angles = 0°, 19.5°, 38.8°, 51.5°, 59.1°

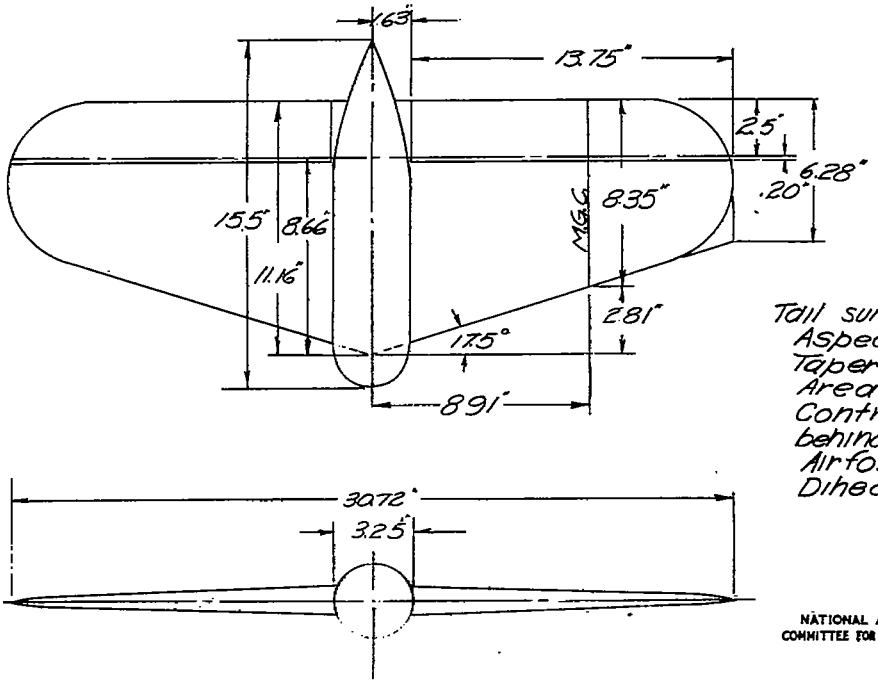

Tail surface B
Aspect ratio = 3.70
Taper ratio = 0.56
Area = 1.78 sq ft
Control-surface area behind hinge line = 0.50 sq ft
Airfoil section, NACA 0009
Dihedral angles = 0°, 30.0°, 39.8°, 50.3°

NATIONAL ADVISORY COMMITTEE FOR AERONAUTICS

Figure 3.- Isolated tail surfaces A and B used in force tests in Langley free-flight tunnel to check vee-tail theory.

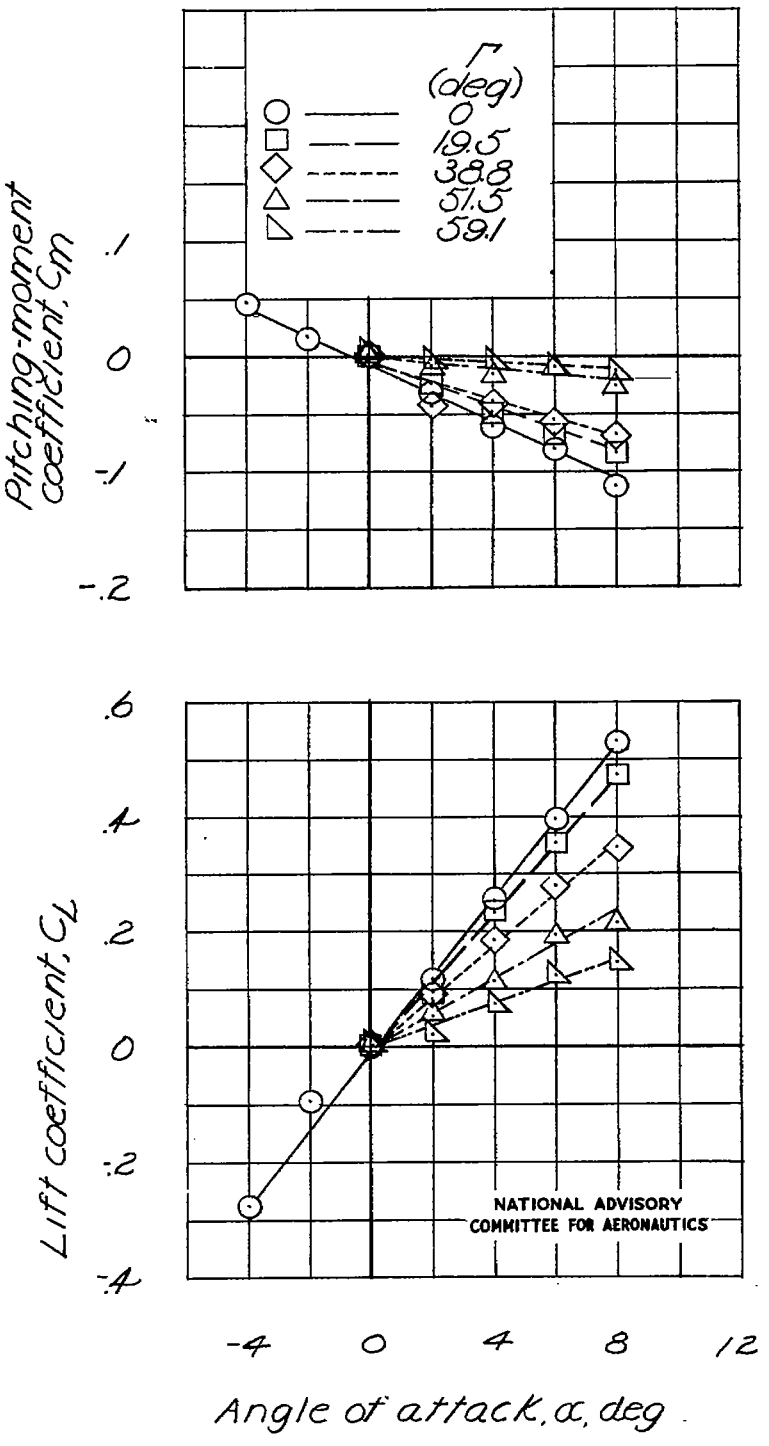

Figure 4.- Lift and pitching-moment characteristics of tail A with various dihedral angles. $\delta_e = \delta_r = \psi = 0°$.

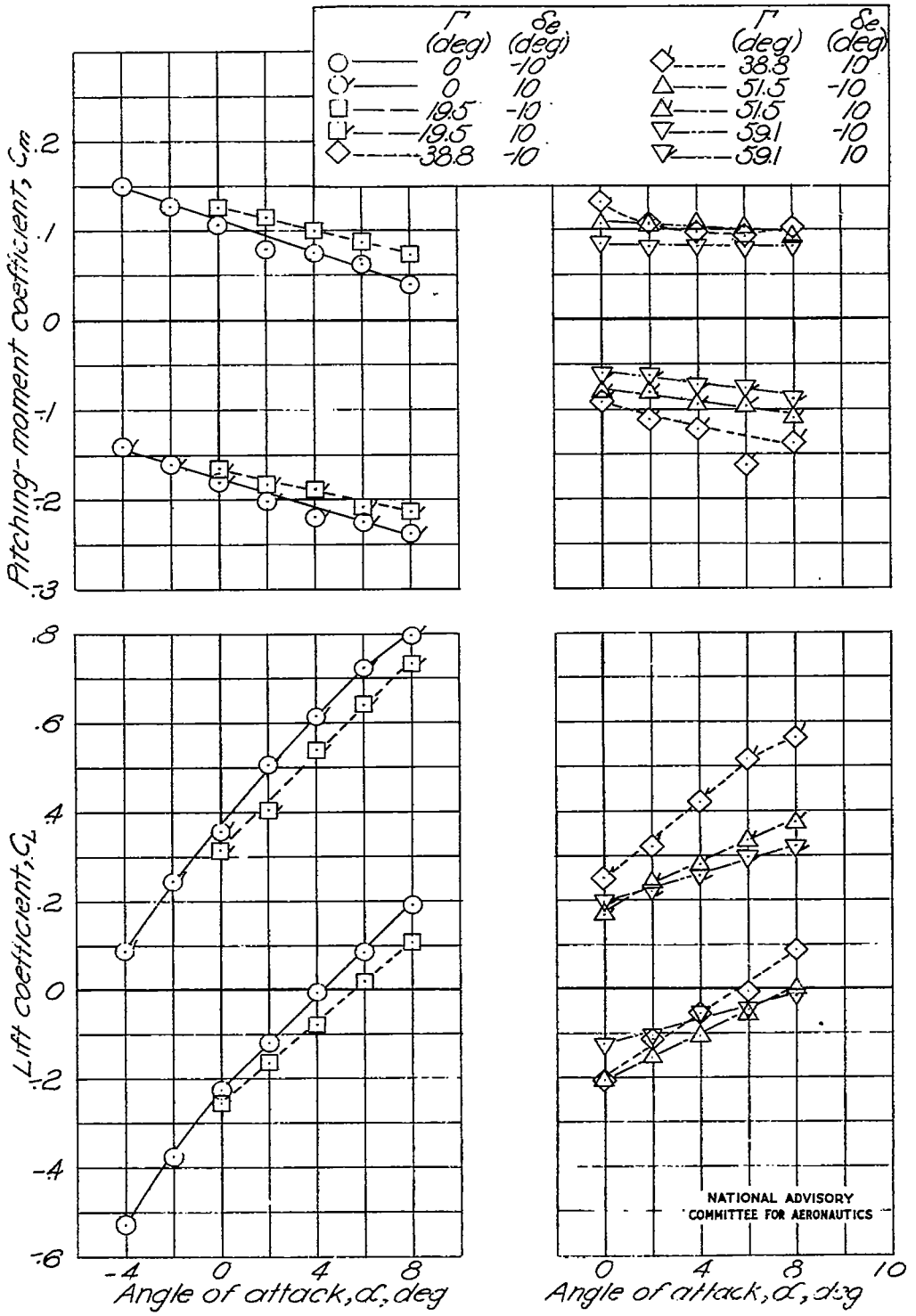

Figure 5.- Elevator effectiveness of tail A with various dihedral angles. $\delta_r = \psi = 0°$.

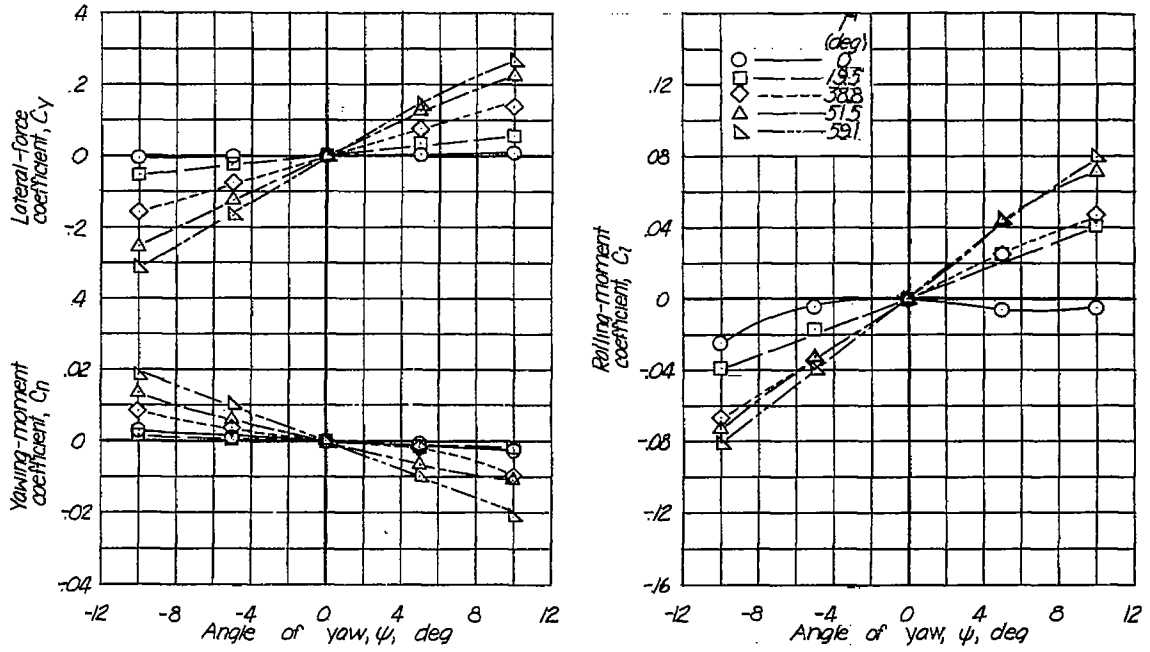

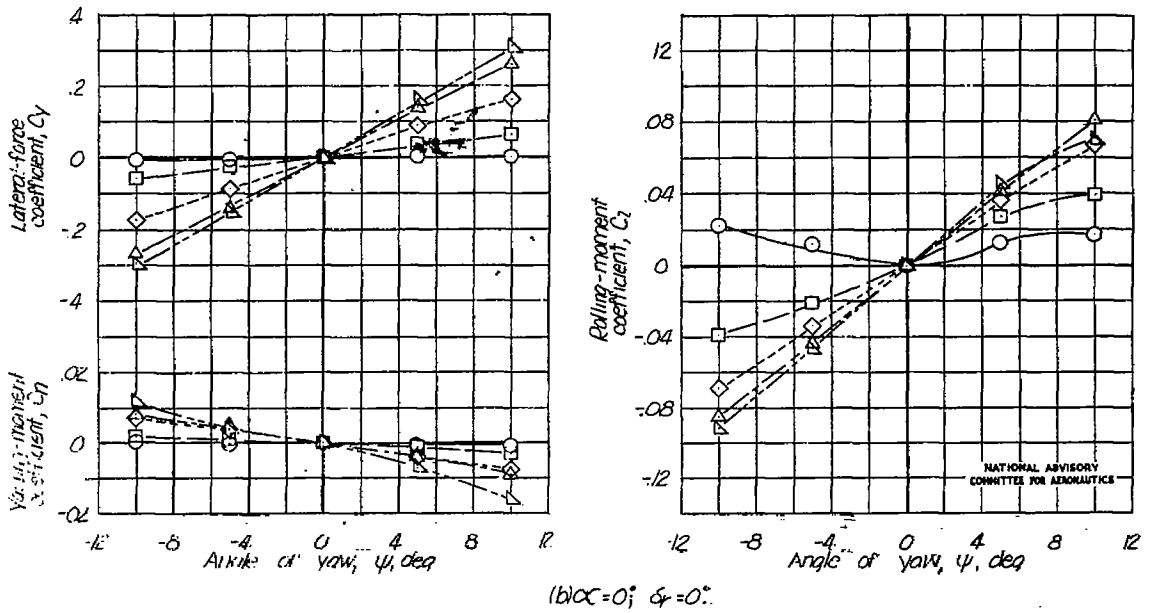

Figure 6.- Rolling-moment, yawing-moment, and lateral-force characteristics of tail A with various dihedral angles. $\delta_e = 0°$.

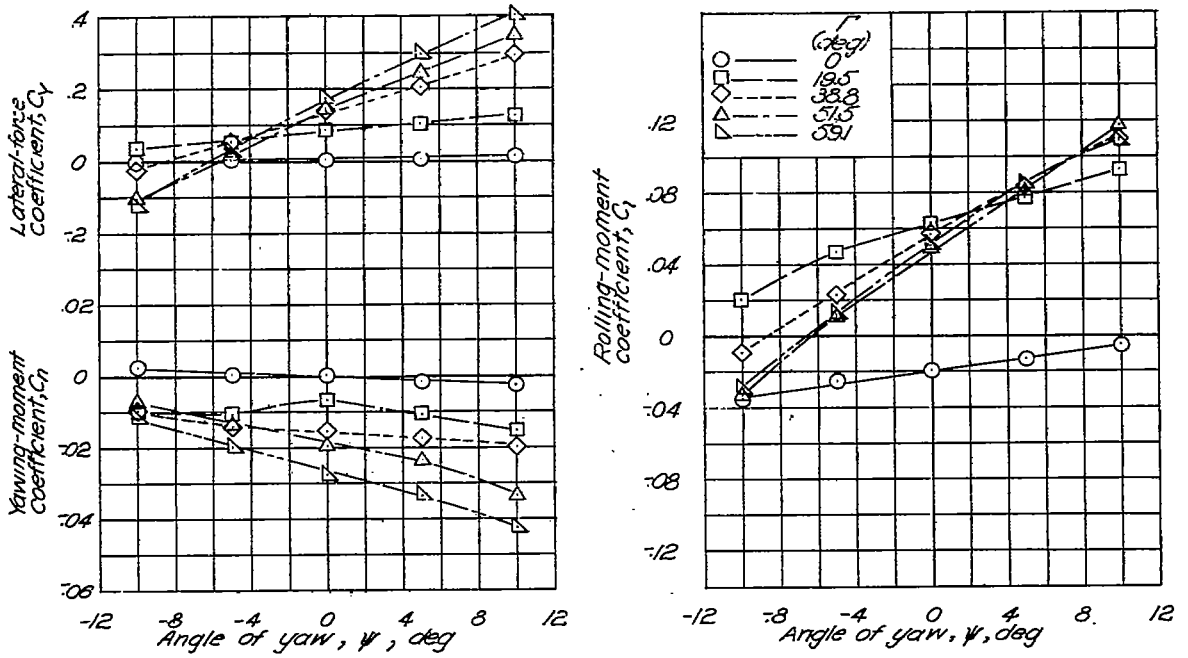

(c) $\alpha = 8°$; $\delta_r = 10°$.

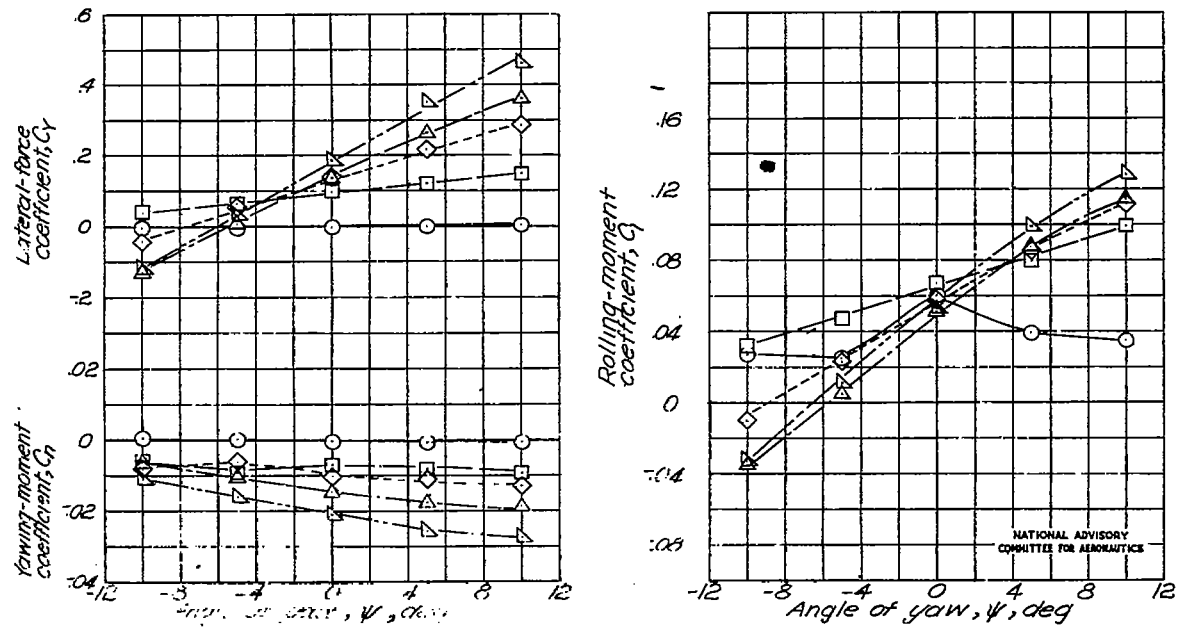

(d) $\alpha = 0°$; $\delta_r = 10°$.

Figure 6.- Concluded.

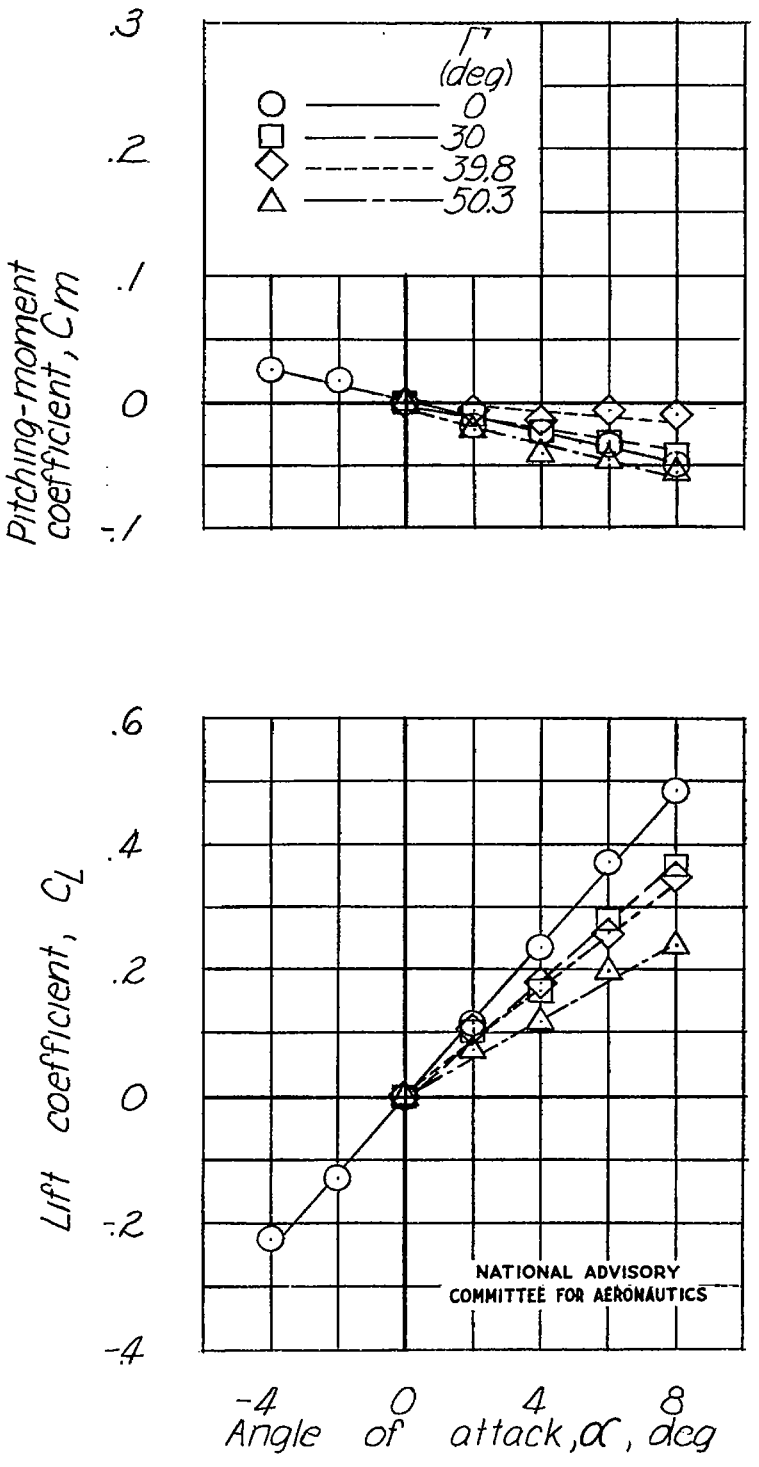

Figure 7.- Lift and pitching-moment characteristics of tail B with various dihedral angles. $\delta_c = \delta_r = \psi = 0°$.

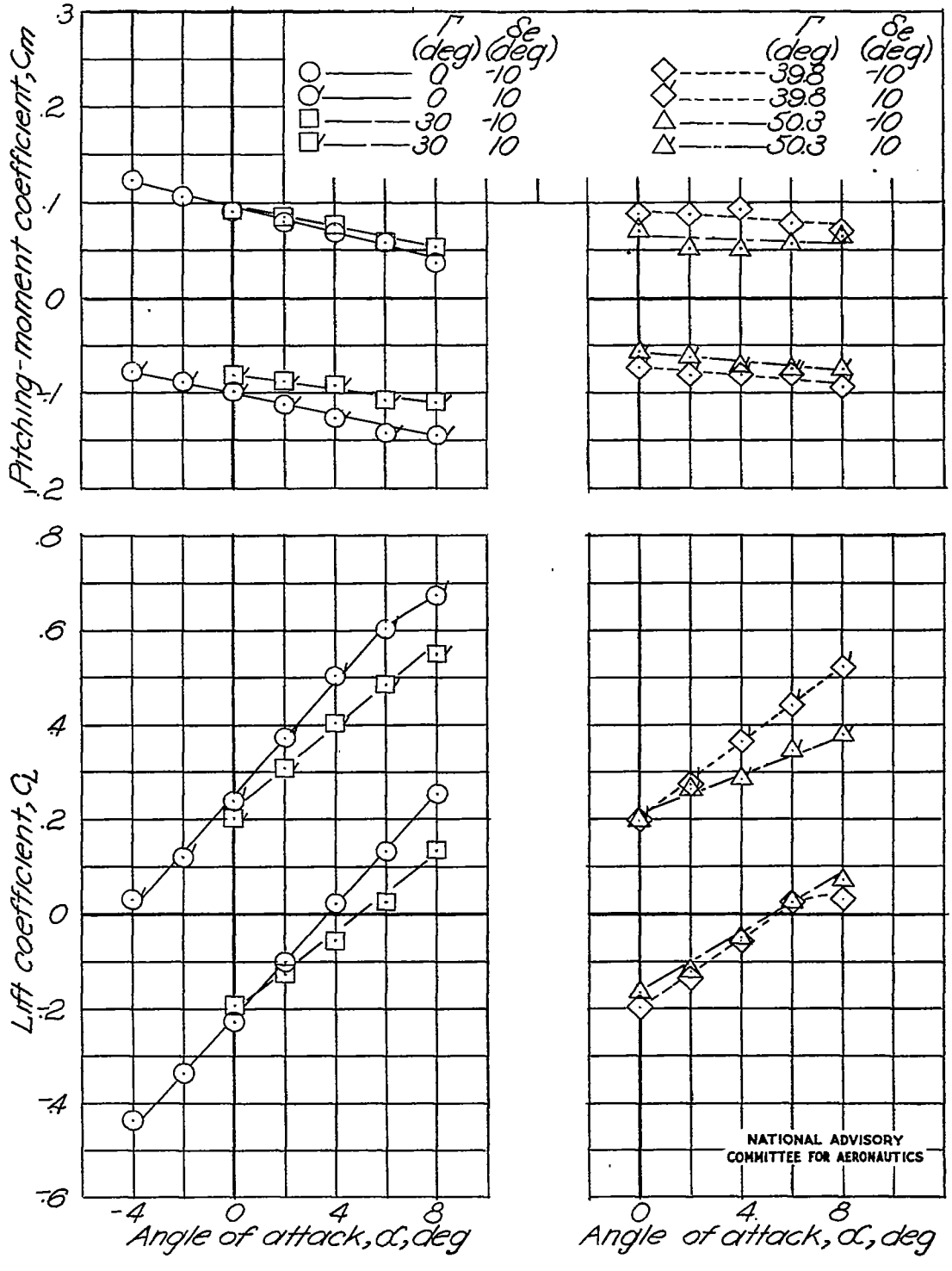

Figure 8.- Elevator effectiveness of tail B with various dihedral angles. $\delta_r = \psi = 0°$.

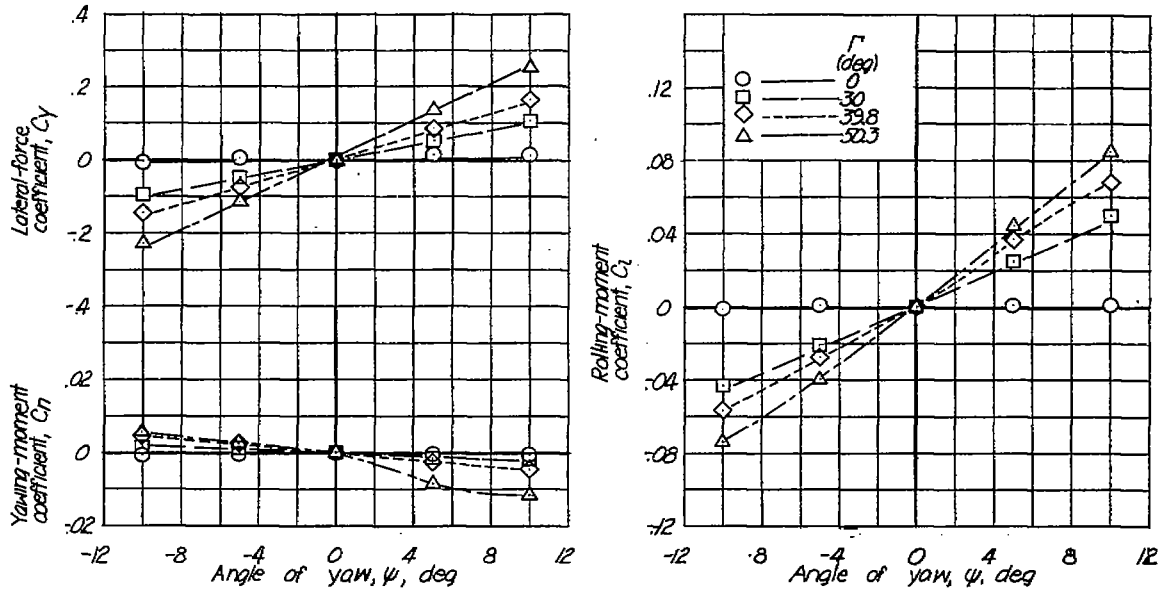

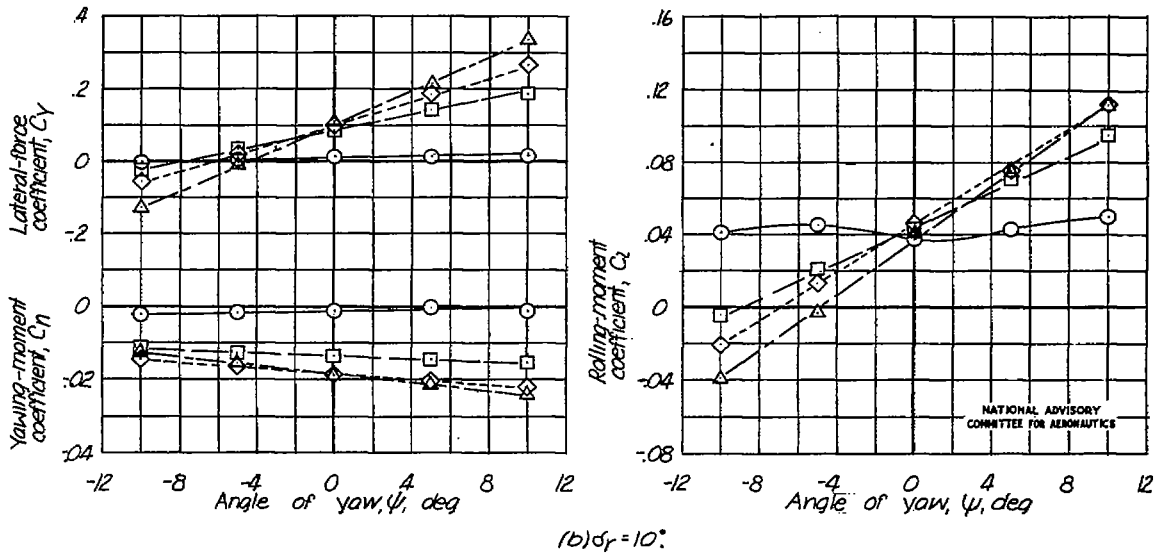

Figure 9.- Rolling-moment, yawing-moment, and lateral-force characteristics of tail B with various dihedral angles. $\delta_e = \alpha_c = 0°$.

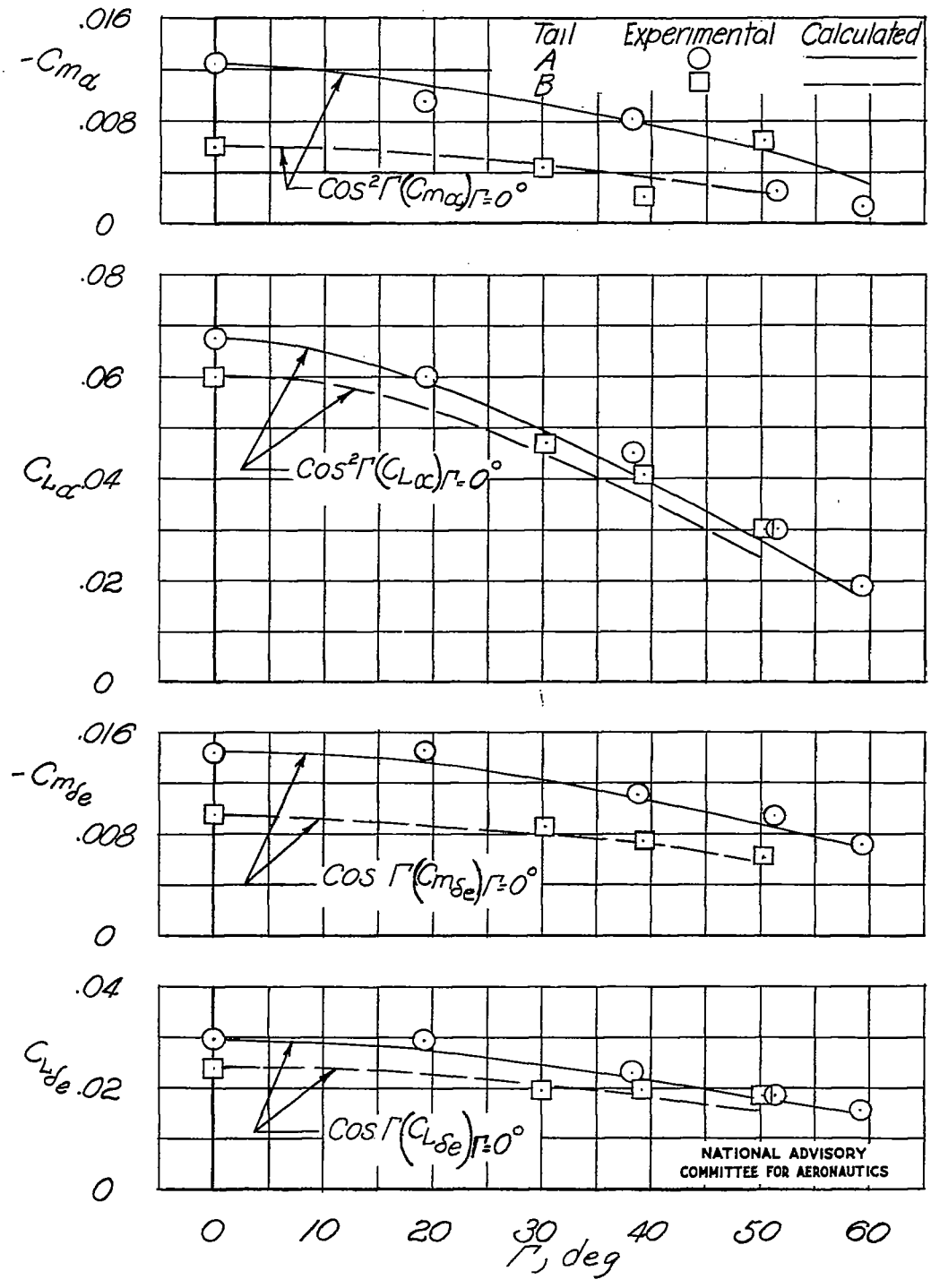

Figure 10.- Variation of lift and pitching-moment parameters with dihedral angle. $\alpha = \delta_r = 0°$.

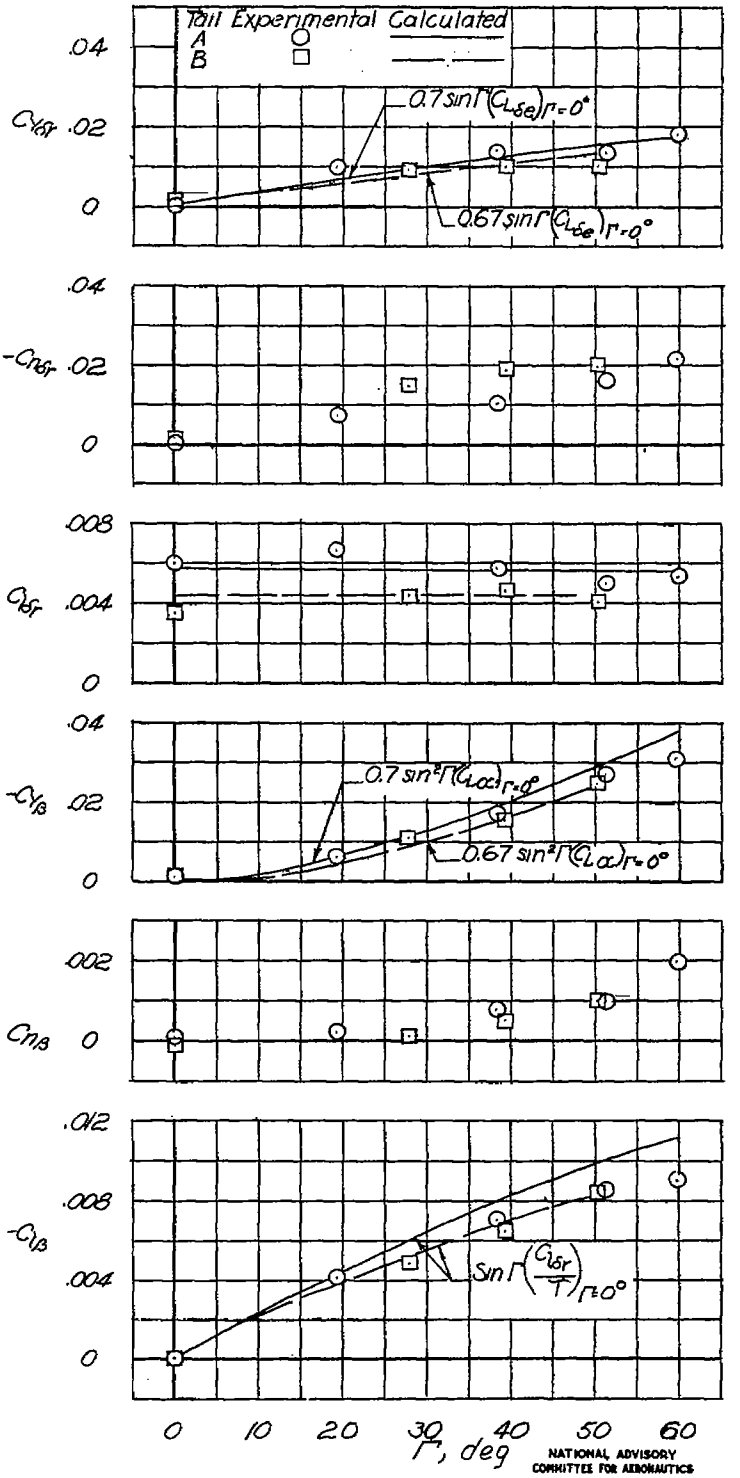

Figure 11.- Variations of rolling-moment, yawing-moment, and lateral-force parameters with dihedral angle. $\alpha = \delta_e = 0°$.